

## Original Article

# Tumor suppressor miR-33b-5p regulates cellular function and acts a prognostic biomarker in RCC

Guocheng Huang<sup>1,2\*</sup>, Yulin Lai<sup>1,3\*</sup>, Xiang Pan<sup>1,4</sup>, Liang Zhou<sup>1</sup>, Jing Quan<sup>1,4</sup>, Liwen Zhao<sup>1,4</sup>, Zuwei Li<sup>1,2</sup>, Canbin Lin<sup>1,2</sup>, Jingyao Wang<sup>1</sup>, Hang Li<sup>1</sup>, Haichao Yuan<sup>1</sup>, Yu Yang<sup>1</sup>, Yongqing Lai<sup>1,2</sup>, Liangchao Ni<sup>1,2</sup>

<sup>1</sup>Guangdong and Shenzhen Key Laboratory of Male Reproductive Medicine and Genetics, Peking University Shenzhen Hospital, Shenzhen 518036, Guangdong, P. R. China; <sup>2</sup>Shantou University Medical College, Shantou 515041, Guangdong, P. R. China; <sup>3</sup>Department of Urology, People's Hospital of Longhua, Shenzhen, Guangdong 518109, P. R. China; <sup>4</sup>Anhui Medical University, Hefei 230032, Anhui, P. R. China. \*Co-first authors.

Received September 28, 2019; Accepted June 19, 2020; Epub July 15, 2020; Published July 30, 2020

**Abstract:** Background: Renal cell carcinoma (RCC) is a renal parenchyma neoplasm with a 30% recurrence rate even when treated properly. MicroRNAs are noncoding small RNAs that are involved in cellular communication and may participate in cancer development. This study aimed to explore the relationship between miR-33b-5p expression and RCC progression and prognosis. Method: RT-qPCR, CCK-8 assay, wound scratch assay, transwell assay and flow cytometry assay were used to evaluate the expression and function of miR-33b-5p in RCC. Additionally, RCC samples and survival data from The Cancer Genome Atlas were used to analyze the prognostic functions of miR-33b-5p. Results: miR-33b-5p expression in RCC tissues and cell lines (786-O, ACHN) were found to be significantly down-regulated, compared with normal tissues and cell lines ( $P < 0.001$ ). The miR-33b-5p mimic transfected cells showed a slower proliferation rate ( $P < 0.01$ ), while its invasion ability decreased by 38.16% (786-O,  $P < 0.001$ ) and 49.19% (ACHN,  $P < 0.05$ ), compared with the negative control (NC). The migration ability of both RCC lines were found to be as follows: miR-33b-5p inhibitor > NC or NC inhibitor > miR-33b-5p mimic. Additionally, TCGA and RCC samples reveal that low miR-33b-5p expression is related to poor survival outcomes (univariate analysis,  $P = 0.029$ ; multivariate analysis,  $P = 0.024$ ; Kaplan-Meier survival curves,  $P = 0.014$ ). Target genes prediction suggests that miR-33b-5p performs its tumor-suppressive effects and prognostic role through targeting TBX15, SLC12A5, and PTGFRN. Conclusions: miR-33b-5p may function as a tumor-suppressive regulator and prognostic biomarker in RCC.

**Keywords:** miR-33b-5p, microRNA, renal cell carcinoma, prognostic biomarker

## Introduction

Renal cell carcinoma (RCC) is a renal parenchyma neoplasm derived from the malignant transformation of proximal renal tubular epithelial cells [1]. An estimated 73,820 new cases and 14,770 deaths from kidney cancer (primarily renal cell carcinomas) were estimated to have occurred in the US in 2019 [2]. Patients may be diagnosed through imaging conducted for non-related purposes, because symptoms are not shown until advanced stages [3]. The classical triad (flank pain, hematuria, and a palpable abdominal mass) is seen in 5-10% of symptomatic patients, while hematuria (50-60%) or flank pain (35-40%) is the most common complain [4]. Surgical excision of the primary neoplasm is the main treatment method

for RCC and is recommended for most patients who can tolerate it. However, the prognosis of surgical treatment depends on histology classification [5] and TNM stage at diagnosis [4, 5]. The 5-year survival rate drops from 95% at stage I to less than 60% at stage III, and further decreasing to 5-20% at stage IV [4]. Additionally, relapse with metastases occurs in about 30% of patients with localized disease after proper treatment [6]. Thus, it is important to identify potential markers for the early detection and better prognosis of RCC.

MicroRNAs (miRNAs) are endogenous noncoding small RNAs that are involved in cellular communication by decreasing the expression of messenger RNAs [7]. The levels of expression of MicroRNAs vary between different tissues

**Table 1.** Clinicopathological features in RCC patients

Characteristics	Number of cases
Mean age range (years)	50 (25-82)
Sexual distinction	
Male/Female	24/14
Tumor stage	
T1/T2/T3+T4	20/14/4
Fuhrman grade	
I/II/III/IV	16/14/4/4
AJCC clinical stages	
I/II/III+IV	18/13/7

pT, primary tumor; AJCC, American Joint Committee on Cancer.

and health states. miRNAs participate in the development of many types of malignant tumors, which allow miRNAs to function as diagnostic biomarkers [8]. Decreased expression of miR-33b has been reported in multiple myeloma, hepatocellular carcinoma, colorectal cancer and breast cancer cells [9-12]. However, no studies on miR-33b in RCC have been reported as yet. Therefore, the purpose of this study is to detect the expression of miR-33b-5p in RCC tissues and cells and identify the effect of miR-33b-5p on the development of RCC, and also identify the relationship between miR-33b-5p expression and clinical pathological variables and overall survival, as determined using TCGA data and further experiments.

## Materials and methods

### Collection of human tissue sample

This study was reviewed and approved by the Ethics Committee of Shenzhen Hospital, Peking University. Each participating patient fully understood and signed an informed consent form. We collected 38 specimens of RCC and adjacent normal tissues from January 2015 to May 2016 at Shenzhen Hospital, Peking University (Shenzhen, China). The tissues obtained were processed in RNeasy (Qiagen GmbH, Hilden, Germany) for 30 minutes and stored in a refrigerator at -80°C until RNA isolation was conducted. The WHO classification of RCC and the American Cancer Federation staging system were used to determine the clinical stages of these samples. The clinical and pathological features of the patients are shown in **Table 1**.

### Formalin-fixed paraffin-embedded (FFPE) tissue specimens

FFPE samples of RCC were obtained from patients who underwent a kidney operation at Shenzhen Hospital, Peking University between 2010 and 2013. The clinicopathological features of each patient was determined based on the 2010 American Joint Committee on Cancer staging system (**Table 3**). Total miRNA of the FFPE samples were extracted using a miRNeasy FFPE Kit (Qiagen).

### Cell culture and cell transfection

In this study, one human embryonic kidney cell line (HK-2) and three human renal carcinoma cell lines (786O, ACHN and Caki-1) were cultured in Dulbecco's modified Eagle's medium (DMEM; Invitrogen Life Technologies, Inc., Carlsbad, CA, USA), combined with 10% fetal bovine serum (FBS; Invitrogen Life Technologies, Inc), 1% antibiotics (100 U/ml penicillin and 100 mg/ml streptomycin; Gibco, Thermo Fisher Scientific) and 1% glutamine. These cells were cultivated in a humidified incubator containing 5% carbon dioxide at 37°C. Mixed liquors made up of 200 µl of Opti-MEM medium (Gibco; Thermo Fisher Scientific, Inc.), 200 pmol of a synthetic miR-33b-5p mimic (Gene Pharma, Suzhou, China), inhibitor, negative control (NC) or inhibitor negative control (NC inhibitor) and 5 µl of Lipofectamine 2000 (Invitrogen; Thermo Fisher Scientific, Inc.). Corresponding experimental tests were subsequently performed. The sequences used are listed in **Table 2**.

### RNA extraction, cDNA synthesis and RT-qPCR

TRIzol reagent was used to extract total RNA from the samples and RNA concentrations were determined using a NanoDrop 2000c system (Thermo Scientific, USA). Total RNA was purified using a RNeasy Maxi kit (Qiagen GmbH). According to the manufacturer's instructions, 1 µg of total RNA and a miRNA Reverse Transcription Kit (Qiagen, Germany) were added to the reaction system for reverse transcription, using a general PCR machine (BIO-RAD, USA). Then, reverse transcription quantitative real-time polymerase chain reaction (RT-qPCR) was performed to detect the expression level of miR-33b-5p using a miScript SYBR®Green

**Table 2.** Sequences of primers and microRNAs

Primer/microRNA	Sequence
miR-33b-5p	Forward: 5'-GTGCATTGCTGTTGCATTGC-3' Reverse: Universal primers (miScript SYBR Green PCR kit)
U6	Forward: 5'-CTCGCTTCGGCAGCACA-3' Reverse: 5'-ACGCTTCACGAATTTGCGT-3'
miR-33b-5p mimic	Forward: 5'-GUGCAUUGCUGUUGCAUUGC-3' Reverse: 5'-AAUGCAACAGCAAUGCACUU-3'
miR-33b-5p inhibitor	5'-GCAAUGCAACAGCAAUGCAC-3'
NC	Forward: 5'-UUCUCCGAACGUGUCACGUTT-3' Reverse: 5'-ACGUGACACGUUCGGAGAATT-3'
NC inhibitor	5'-CAGUACUUUUGUGUAGUACAA-3'

miR, microRNA; NC, negative control; PCR, polymerase chain reaction.

to the wells and the cells were incubated in the dark at 37°C for 30 minutes in a humidified incubator containing 5% CO<sub>2</sub>. Then, an ELISA microplate reader (Bio-Rad Laboratories Inc., Hercules, CA, USA) was used to determine the OD of each well of different cell groups at an absorbance of 490 nm.

#### Wound scratch assay

**Table 3.** Association between miR-33b-5p expression level<sup>1</sup> and Clinical information in FFPE renal cancer samples

Variable	Total	No. of patients (%)		P-value <sup>2</sup>
		High	Low	
Gender				
Male	26	10	16	0.111
Female	16	11	5	
Age (Years)				
≤ 60	33	16	17	1.000
> 60	9	5	4	
Tumor size (cm)				
≤ 4.0	17	7	10	0.530
> 4.0	25	14	11	
Tumor stage				
I+II	27	14	13	1.000
III+IV	15	7	8	

<sup>1</sup>cut-off point: median. <sup>2</sup>calculated using Fisher's Exact test or Pearson Chi-square test.

PCR kit (Qiagen GmbH) on a Roche Lightcycler 480 Real-Time PCR system (Roche Diagnostics, Basel, Switzerland). U6 snRNA was used as an internal reference gene. The 2<sup>-ΔΔCq</sup> method was used to analyze miR-33b-5p expression levels.

#### Cell counting kit-8 (CCK-8) assay

Proliferation of 786-O cells and ACHN cells were assessed using a CCK-8 assay. Each 96-well plate was divided into four groups, based on experimental requirements, with 5000 transfected cells in each well. At 0, 24, 48 and 72 hours post-transfection, 10 μl of the Cell Counting Kit-8 (Everbright Inc., USA) was added

The wound scratch assay was designed to evaluate the mobility of 786-O and ACHN cells. Images of the cells were captured using a digital camera system (Olympus Corporation, Tokyo, Japan) at 0 h and 24 h.

#### Transwell assay

The transwell assay was designed to evaluate the migration and invasion abilities of 786-O and ACHN cells. Transwell chamber inserts (BD Biosciences, Franklin Lakes, NJ, USA) with (for invasion) or without Matrigel (BD Biosciences) were used in the transwell assay, according to the manufacturer's instructions. 3 × 10<sup>4</sup> transfected cells were diluted in 200 μl of serum-free DMEM. The different groups of cells were inoculated in the upper chamber and DMEM containing 10% FBS medium was added to the lower chamber. The 786-O cell culture underwent 36 hours of migration and 48 hours of invasion, while the ACHN cell culture underwent 36 hours of migration and 60 hours of invasion. After staining with crystal violet, the cells were observed under a microscope and cell numbers in five different fields of view were counted.

#### Flow cytometry assay

The apoptosis rate of 786-O cells and ACHN cells were evaluated using flow cytometry. 3 × 10<sup>5</sup> cells were seeded into each well of a 6-well plate. Each experimental group of cells was transfected with 200 pmol of a miR-33b-5p mimic, inhibitor, negative control (NC) or inhibitor negative control (NC inhibitor). After the cells were transfected for 48 hours, the cells

collected were washed with PBS two times and were blended with 100  $\mu$ l of a 1  $\times$  binding buffer. 5  $\mu$ l of Annexin V-fluorescein isothiocyanate (Invitrogen; Thermo Fisher Scientific, Inc.) and 5  $\mu$ l of propidium iodide (Invitrogen; Thermo Fisher Scientific, Inc.) were added to the cell resuspension. After staining for 15 minutes at room temperature, 400  $\mu$ l of a 1  $\times$  binding buffer was added into each tube. The apoptosis rate was analyzed using a flow cytometer (EPLCS XL 4; Beckman Coulter, Inc., Brea, CA, USA).

## Survival analyses using TCGA database

In order to explore the prognostic functions of miR-33b-5p in RCC, survival data was obtained from The Cancer Genome Atlas (TCGA <https://cancergenome.nih.gov/>). miR-33b-5p data was entered onto OncoLnc (<http://www.oncolnc.org/>) for survival analyses. 506 RCC patients from TCGA were enrolled in our study. The patients were divided into two groups (50%, high expression; 50%, low expression) and were evaluated using Kaplan-Meier analysis.

## TCGA database analysis and targets prediction of miR-33b-5p

The clinical manifestations and sequencing data of RCC samples and paired normal samples were obtained from the TCGA database. With LIMMA differential methods, the differential expressed genes (DEGs) of RCC were defined by  $|\text{Log}_2 \text{ Fold Change}| > 1$ , adjusted  $p$ -value  $< 0.01$ . Target genes of miR-33b-5p were predicted by TargetScan (v7.0; [targetscan.org](http://targetscan.org)) [13]. The predicted target genes of miR-33b-5p were matched with the up-regulated DEGs of RCC. Additionally, the TCGA database was used for expression analysis and survival analysis of the matched DEGs by GEPIA (<http://gepia.cancer-pku.cn/index.html>).

## Statistical analysis

All data are expressed as mean  $\pm$  standard error and data processing was conducted using SPSS 19.0 (SPSS, Armonk, NY, USA) software. Paired  $t$ -tests were used to compare differences in miR-33b-5p expression between renal cell carcinoma tissues and paracancerous tissues. Student's  $t$ -test, Fisher's exact test or Pearson chi-square test were used to analyze the relationship between miR-33b-5p expression and clinicopathological parameters. Stu-

dent's  $t$ -test was also used to analyze cell phenotypes. Additionally, Cox proportional hazards regression analysis was used to determine univariate and multivariate levels of miR-33b-5p expression and clinical pathological variables or survival. Survival curves were drawn using Kaplan-Meier curves and differences between these curves were assessed using the log-rank test. A  $P$  value of  $< 0.05$  was considered statistically significant.

## Results

### miR-33b-5p was downregulated in RCC tissues and cell lines

We collected RCC tissues and adjacent normal tissues from 38 cases to detect the expression level of miR-33b-5p (**Figure 1A**). The results show that the expression of miR-33b-5p in RCC tissues is significantly downregulated, compared with adjacent normal tissues ( $P < 0.001$ , **Figure 1B**). Similarly, the results of RCC cell lines show that relative miR-33b-5p expression levels are significantly downregulated in 786-O ( $P < 0.001$ ), ACHN ( $P < 0.001$ ) and Caki-1 ( $P < 0.001$ ) cells, compared with that of HK-2 cells (**Figure 1C**). In brief, the expression of miR-33b-5p in RCC tissues and RCC cell lines (786-O, ACHN and Caki-1 cell) is significantly downregulated, compared with adjacent normal tissues and normal cell lines (HK-2 cells).

### Validation of cell transfection efficiency

RT-qPCR was used to confirm the transfection efficiency of the miR-33b-5p mimic and miR-33b-5p inhibitor. miR-33b-5p expression levels of transfected cells were compared with their respective NC in the 786-O and ACHN cell lines (**Figure 1D**). As expected, miR-33b-5p relative expression levels were as follows: miR-33b-5p mimic  $>$  NC and NC inhibitor  $>$  miR-33b-5p inhibitor, in both 786-O and ACHN cell lines. These cell lines were used to explore the functions of miR-33b-5p in cell proliferation, migration, invasion and apoptosis.

### miR-33b-5p inhibits cell proliferation

Cell proliferation is reflected by optical density (OD) values detected in a CCK-8 assay. Higher OD values indicate faster proliferation. Our experiment was designed to explore the relationship between miR-33b-5p expression lev-

## Tumor suppressor miR-33b-5p in renal cell carcinoma

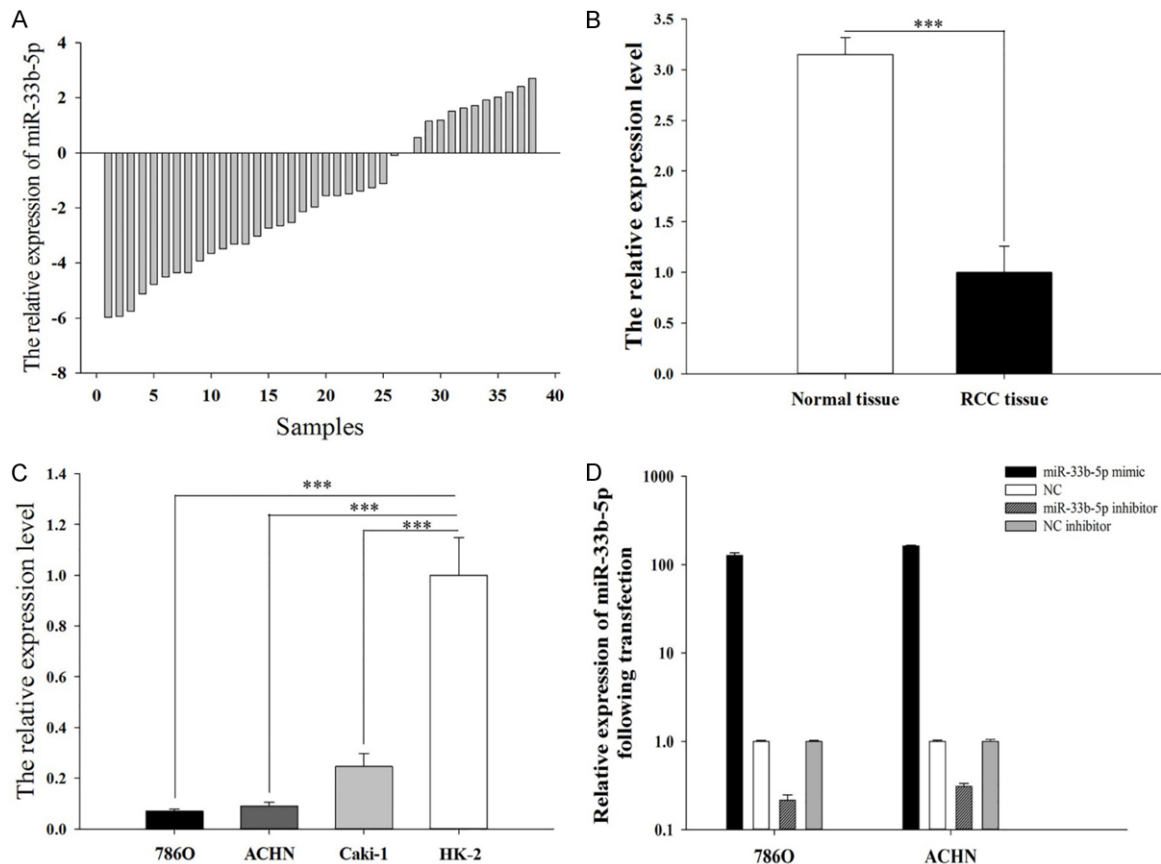


**Figure 1.** The relative expression level of miR-33b-5p in different tissues and cell lines. A. Logarithmic ratio of miR-33b-5p expression in 38 paired RCC tissues (T) with normal kidney tissues (N) [ $\log_2 (T/N)$ ]. B. The mean expression of miR-33b-5p in RCC tissues is significantly down-regulated than adjacent normal tissues. C. The relative expression levels of miR-33b-5p in HK-2 cell is significantly higher than that in 786-O cell, ACHN cell, or Caki-1 cell. D. The relative expression levels of miR-33b-5p in 786-O and ACHN cell lines after transfection with miR-33b-5p mimic, inhibitor, NC and NC inhibitor. \*\*\* $P < 0.001$ ; NC, negative control.

els and the cell proliferation rate. Results from 786-O cells show that the proliferation rate slows down by 15.74% ( $P < 0.01$ ), 18.26% ( $P < 0.01$ ) and 16.44% ( $P < 0.05$ ) in the miR-33b-5p mimic group (**Figure 2A**), compared with the NC at 24, 48 and 72 hours, respectively, while it accelerated by 31.44% ( $P < 0.01$ ), 41.65% ( $P < 0.01$ ) and 21.57% ( $P < 0.01$ ) in the miR-33b-5p inhibitor group (**Figure 2B**), compared with NC inhibitor at 24, 48 and 72 hours, respectively. A similar result was obtained using ACHN cells, with a higher expression level of miR-33b-5p found to be correlated with a lower cell proliferation rate. Results obtained using ACHN cells show that the proliferation rate slowed down by 18.00% ( $P < 0.05$ ), 16.92% ( $P < 0.01$ ), 27.96% ( $P < 0.001$ ) in miR-33b-5p mimic group (**Figure 2C**), compared with NC at 24, 48 and 72 hours, respectively, while it accelerated by

14.67% ( $P < 0.05$ ), 22.62% ( $P < 0.01$ ) and 24.41% ( $P < 0.01$ ) in miR-33b-5p inhibitor group (**Figure 2D**) compared with NC inhibitor at 24, 48 and 72 hours, respectively. All these results indicate that the overexpression miR-33b-5p suppresses RCC proliferation.

### miR-33b-5p inhibits cell mobility

We used wound scratch assay and transwell assay to measure cell mobility. Specifically, wound scratch assay was used to detect cell migration ability (**Figure 3**), while transwell assay was used to assess both migration and invasion abilities (**Figure 4**). As shown in **Figures 3 and 4**, the migration ability of both 786-O and ACHN cell lines were found to be as follows: miR-33b-5p inhibitor > NC and NC inhibitor > miR-33b-5p mimic, which is opposite to the

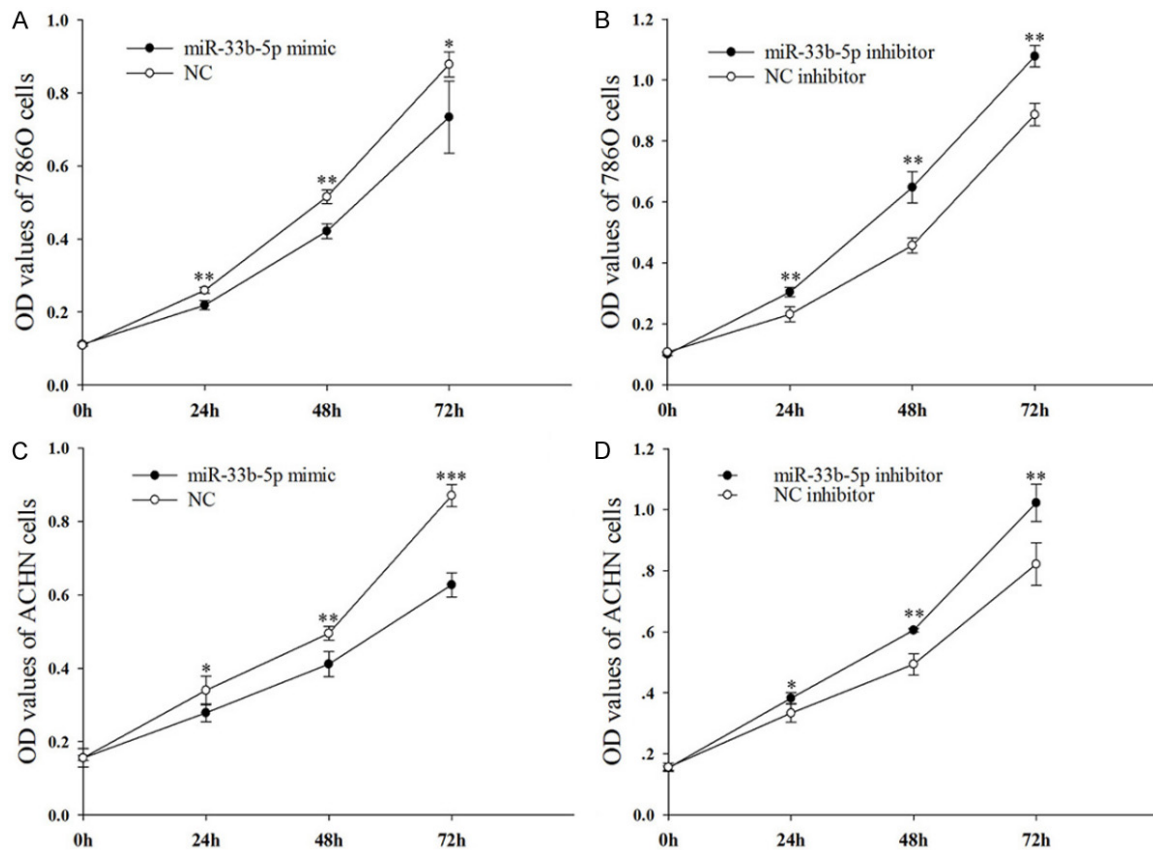


**Figure 2.** Cell proliferation was measured by CCK-8 assay at different time intervals. OD values of 786-O cells and ACHN cells in different time intervals after transfection with miR-33b-5p mimic or miR-33b-5p inhibitor. A, C. OD values of 786-O cells and ACHN cells are significantly up-regulated after transfection with miR-33b-5p mimic. B, D. OD values of 786-O cells and ACHN cells are significantly down-regulated after transfection with miR-33b-5p inhibitor. \* $P < 0.05$ , \*\* $P < 0.01$ , \*\*\* $P < 0.001$ . NC, negative control; OD, optical density; CCK-8, Cell Counting Kit 8.

trend detected for miR-33b-5p expression level. In 786-O and ACHN cell lines, the migration distance of miR-33b-5p mimic transfected cells was significantly 55.61% and 40.45% shorter than that of NC cells (786-O cell line,  $P < 0.01$ ; ACHN cell line,  $P < 0.001$ ), while the migration distance of miR-33b-5p inhibitor transfected cells was 87.56% and 55.96% longer than that of NCin cells (786-O cell line,  $P < 0.01$ ; ACHN cell line,  $P < 0.01$ ). Similar results were obtained from the transwell assay (Figure 4A and 4C). For the 786-O and ACHN cell lines, the migration ability of miR-33b-5p mimic transfected cells was found to have significantly decreased by 45.25% and 50.58%, compared with that of NC cells (786-O cell line,  $P < 0.01$ ; ACHN cell line,  $P < 0.001$ ), while the migration ability of miR-33b-5p inhibitor transfected cells was found to have significantly increased by 80.08% and 72.55%, compared with that of NC in cells (786-O cell line,  $P < 0.01$ ; ACHN cell

line,  $P < 0.01$ ). These results suggest that the upregulation of miR-33b-5p inhibits RCC cell migration. In addition, the invasion ability of miR-33b-5p mimic transfected cells was found to decreased by 38.16% (786-O,  $P < 0.001$ ) and 49.19% (ACHN,  $P < 0.05$ ), compared with NC cells, while the invasion ability of miR-33b-5p inhibitor transfected cells was found to increase by 80.47% (786-O,  $P < 0.01$ ) and 100.9% (ACHN,  $P < 0.001$ ), compared with inhibitor NC cells (Figure 4B and 4D). These results suggest that the upregulation of miR-33b-5p inhibits the invasive ability of RCC cells. Altogether, our results suggest that the overexpression of miR-33b-5p inhibits RCC cell migration and invasion.

#### miR-33b-5p induces cell apoptosis

As shown in Figure 5, the apoptosis rate of miR-33b-5p mimic transfected cells increased by

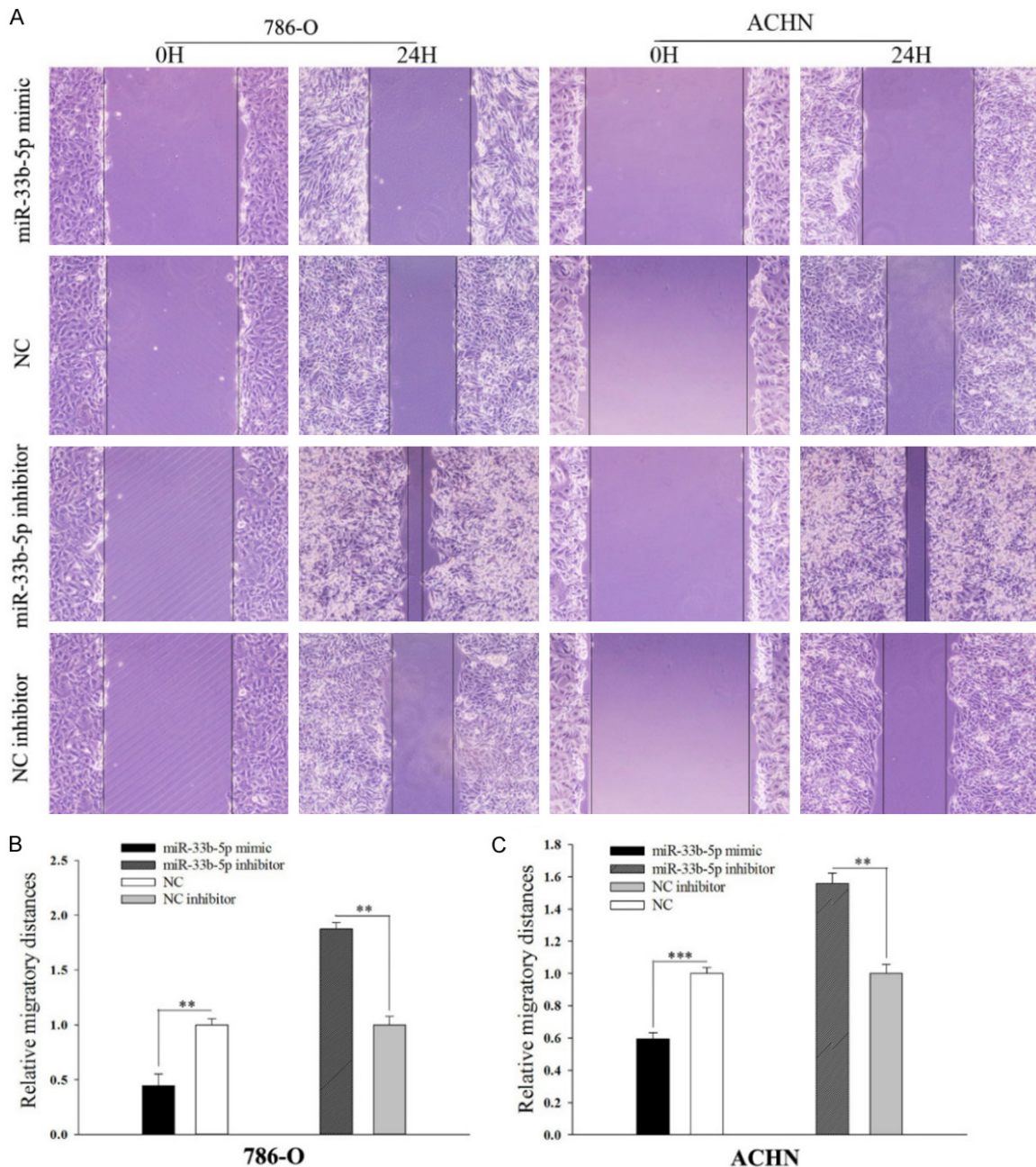


**Figure 3.** The wound healing assay was designed to measure cell migration ability. (A) The wound healing images in 786-O and ACHN cells. The relative migratory distance of miR-33b-5p mimic transfected cell is decreased, while the relative migratory distance of miR-33b-5p inhibitor transfected cell is increased both in (B) 786-O cell and (C) ACHN cell. \* $P < 0.05$ , \*\* $P < 0.01$ , \*\*\* $P < 0.001$ . NC, negative control.

93.77% in the 786-O cell line (Figure 5A,  $P < 0.01$ ) and 76.72% in the ACHN cell line (Figure 6A,  $P < 0.01$ ), compared to the NC. In contrast, the apoptosis rate of miR-33b-5p inhibitor transfected cells declined by 60.06% in the 786-O cell line (Figure 5B,  $P < 0.01$ ) and 48.52% in the ACHN cell line (Figure 6B,  $P < 0.01$ ), compared with the inhibitor NC. In other words, upregulation of miR-33b-5p correspon-

ded with the increase of the rate of RCC cell apoptosis.

*miR-33b-5p improves the survival probability of RCC patients, indicating that it may be a potential independent prognostic marker for RCC*

The results of the FFPE RCC sample analysis is shown in Table 3. No significant correlation was

# Tumor suppressor miR-33b-5p in renal cell carcinoma

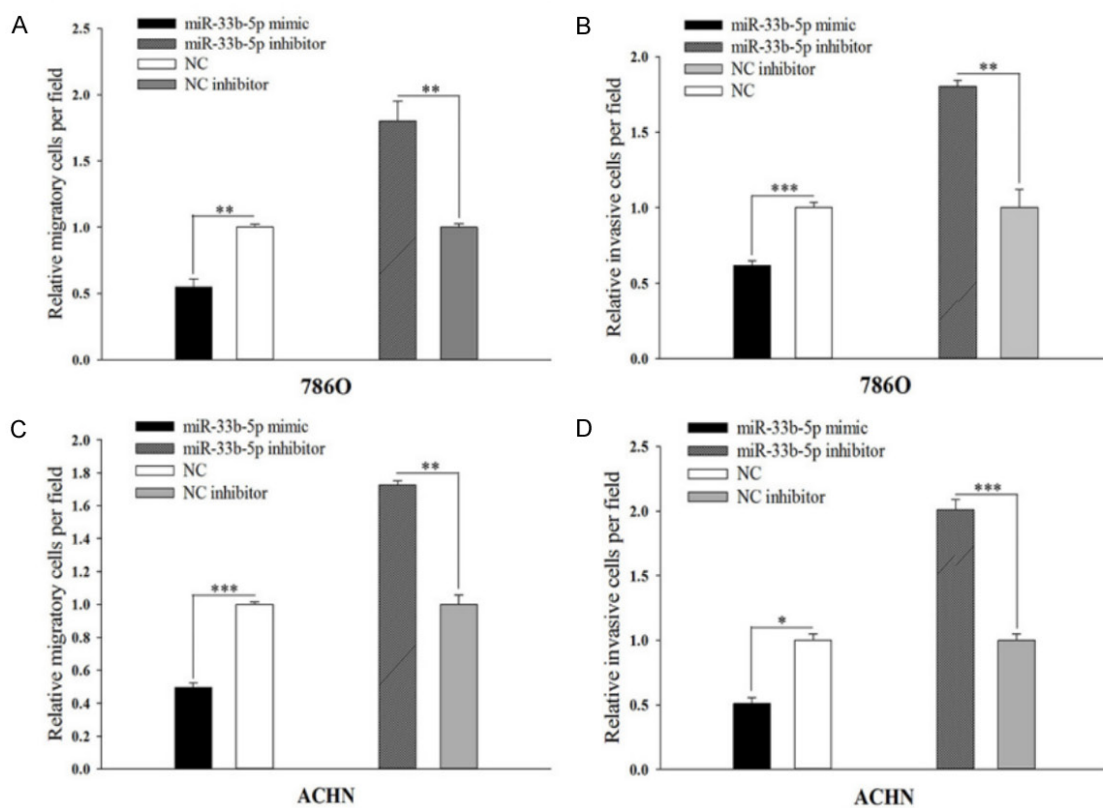
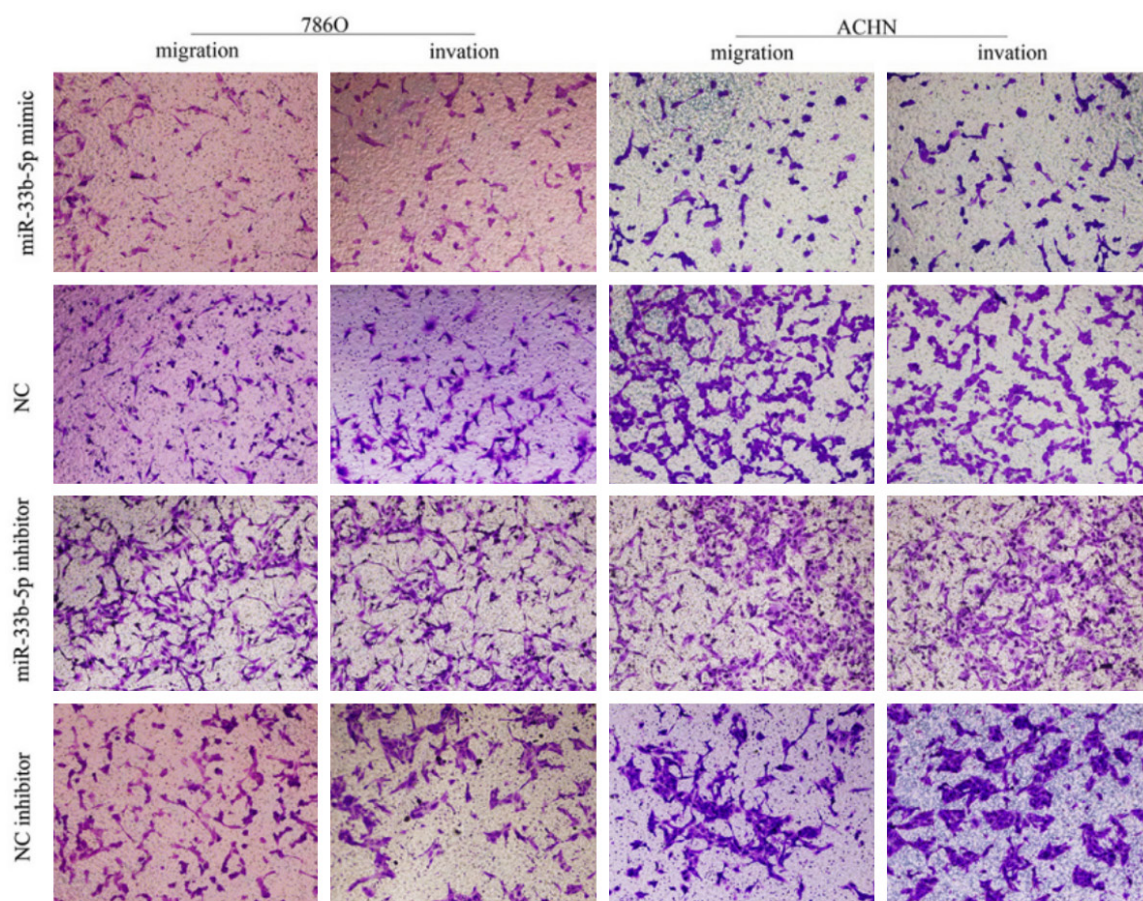


**Figure 4.** Result of the transwell assay. The migratory and invasive images in 786-O and ACHN cells. The relative number of the migratory and invasive cells are significantly decreased in miR-33b-5p mimic transfected cells. Additionally, the relative number of the migratory and invasive cells are significantly increased in miR-33b-5p inhibitor transfected cells. \* $P < 0.05$ , \*\* $P < 0.01$ , \*\*\* $P < 0.001$ . NC, negative control.

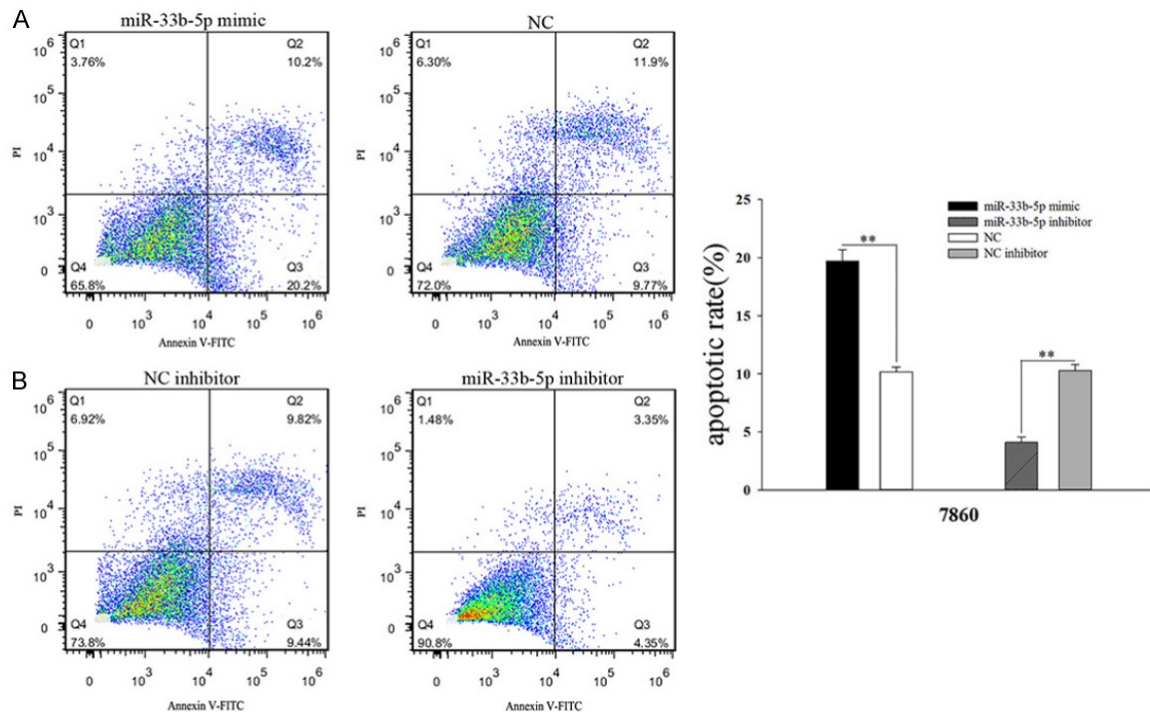


**Figure 5.** The apoptosis rate was measured by flow cytometry assay. Cell distribution of 786-O: survival cells distributed in Q4 while dead cells distributed in Q3. The relative apoptotic rate of 786-O cell is significantly increased after transfection with miR-33b-5p mimic. While the relative apoptotic rate of 786-O cell is significantly decreased after transfection with miR-33b-5p inhibitor. \* $P < 0.05$ , \*\* $P < 0.01$ , \*\*\* $P < 0.001$ . NC, negative control.

found between the expression of miR-33b-5p and other clinicopathologic variables, such as sex, age, tumor size and tumor stage. We used univariate analysis, multivariate analysis and Kaplan-Meier survival curve analysis to assess the relationship between miR-33b-5p expression levels and the survival situation of the RCC patients. The results of the Cox proportional hazards regression analysis are presented in **Table 4**. As shown in **Figure 7A**, the overall survival of high miR-33b-5p expression patients was found to be significantly higher than that of low miR-33b-5p expression patients in the univariate analysis (HR=5.693, 95% CI=1.197-27.067,  $P=0.029$ , **Table 4**). Additionally, as shown in **Figure 7B**, patients with high miR-33b-5p expression also had significantly better survival rates than patients with low miR-33b-5p expression in the multivariate analysis (HR=10.433, 95% CI=1.359-80.089,  $P=0.024$ , **Table 4**). All these results indicate that the over-

expression of miR-33b-5p is related to a higher survival probability (univariate analysis,  $P=0.029$ ; multivariate analysis,  $P=0.024$ ; and Kaplan-Meier survival curves,  $P=0.014$ ; **Figure 7A-C**, respectively).

#### Prediction of miR-33b-5p target genes associated with RCC

2957 DEGs of RCC are obtained by TCGA database analysis. Additionally, 545 target genes of miR-33b-5p are predicted by TargetScan. After matching with up-regulated DEGs, 21 genes are predicted (**Table 5**). Further survival analysis reveals that the up regulation of TBX15, SLC12A5, and PTGFRN are closely related to the poor overall survival of RCC patients (**Figure 8**). Thus, we speculate that miR-33b-5p performs its tumor-suppressive effects and prognostic role through targeting TBX15, SLC12A5, and PTGFRN.

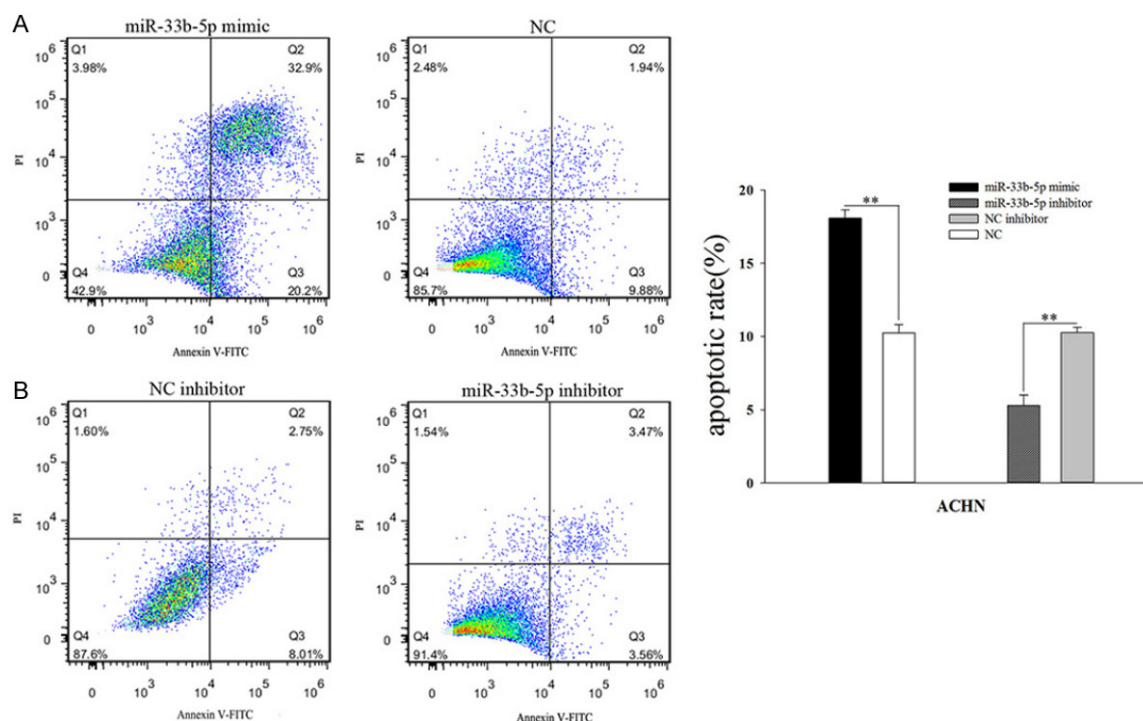


**Figure 6.** The apoptosis rate was measured by flow cytometry assay. Cell distribution of ACHN: survival cells distributed in Q4 while dead cells distributed in Q3. The relative apoptotic rate of ACHN cell is significantly increased after transfection with miR-33b-5p mimic. While the relative apoptotic rate of ACHN cell is significantly decreased after transfection with miR-33b-5p inhibitor. \* $P < 0.05$ , \*\* $P < 0.01$ , \*\*\* $P < 0.001$ . NC, negative control.

**Table 4.** miR-33b-5p expression and patients' survival

Variable	Univariate analysis		Multivariate analysis	
	HR (95% CI)	P-value	HR (95% CI)	P-value
Gender (Female vs Male)	0.352 (0.075-1.662)	0.187	0.240 (0.039-1.477)	0.124
Age ( $\leq 60$ y vs $> 60$ y)	0.304 (0.085-1.081)	0.066	0.126 (0.019-0.832)	0.031
Tumor size ( $\leq 4.0$ cm vs $> 4.0$ )	1.685 (0.486-5.836)	0.411	1.421 (0.323-6.256)	0.642
Tumor stage (I+II vs III+IV)	0.193 (0.050-0.749)	0.017	0.239 (0.049-1.163)	0.076
miR-33b-5p (low vs high)	5.693 (1.197-27.067)	0.029	10.433 (1.359-80.089)	0.024

HR, Hazard ratio; 95% CI, 95% Confidence interval.

## Discussion

Over the past decade, increasing evidence has shown that miRNAs are closely related to the pathogenesis of cancer and survival outcomes of patients [14]. Increased expression of oncogenic miRNAs or a decrease in the expression of antioncogenic miRNAs can contribute to the progression of tumors [15], while some miRNAs have an impact on the effectiveness treatment [16]. A study by Fan et al. suggest that miR-17-92 expression is associated with advanced gastric cancer progression and oxaliplatin/capecitabine chemotherapy effectiveness [17]. Hagstrom et al. demonstrated that breast can-

cer survivors with a high response to resistance training exhibited higher miR-133a-3p expression and a borderline statistically significant increase in the expression of miR-370-3p [18]. Furthermore, Noorolyai et al. concluded that several microRNAs (including miR-21, miR-17-5p, miR-106a and miR-1) participate in the PI3-kinase signaling pathway in colorectal cancer [19].

RCC is the most common renal neoplasia with early metastasis and poor prognosis, which makes research on RCC crucial. Many recent studies have shown that abnormally expressed miRNAs can be used as early diagnosis and

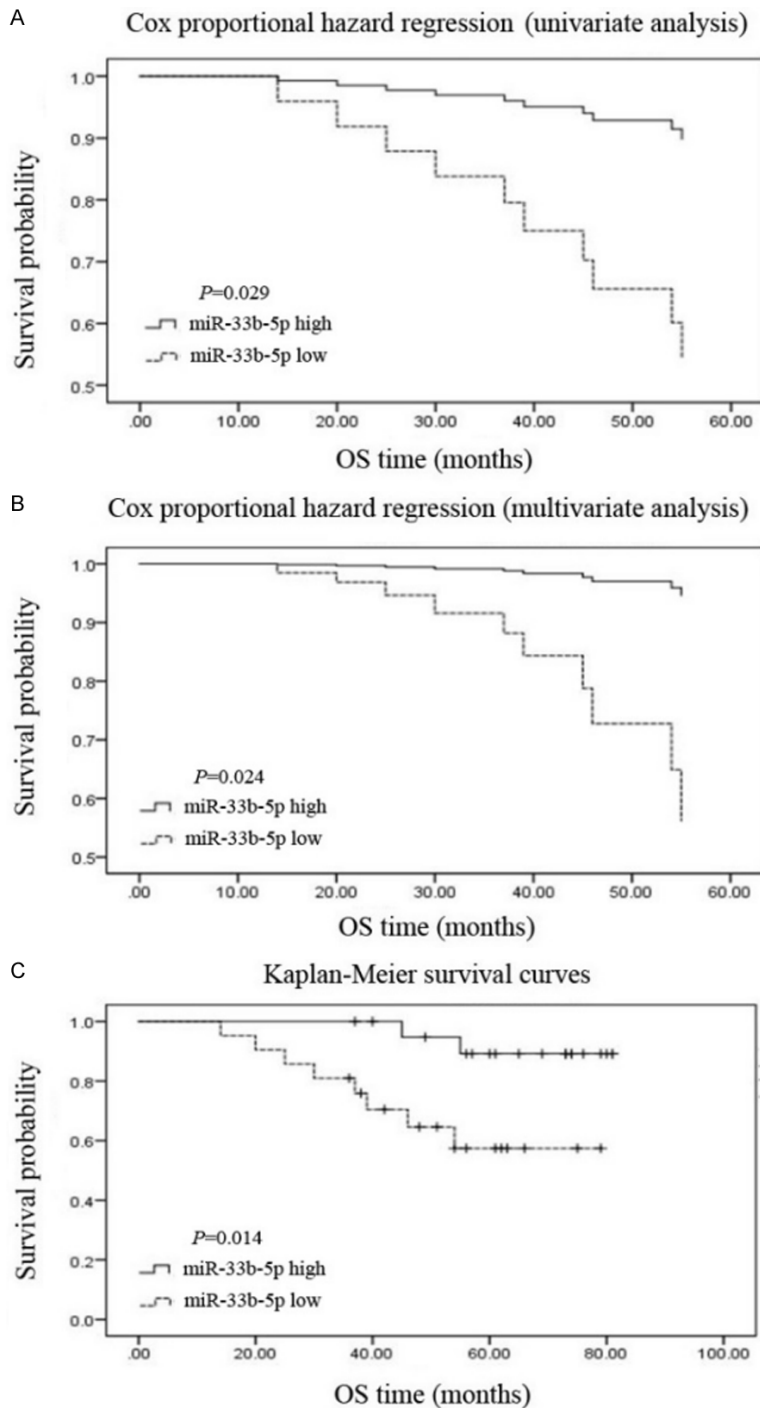


**Figure 7.** Result of survival analysis by FFPE RCC samples. miR-33b-5p expression level is significantly related to patients' survival rate both in (A) the univariate and (B) the multivariate analysis. (C) Patients with high miR-33b-5p expression levels tend to have a higher survival rate in the Kaplan-Meier survival curves. \* $P<0.05$ , \*\* $P<0.01$ , \*\*\* $P<0.001$ . NC, negative control.

prognostic markers of RCC. For example, Iwamoto et al. have revealed that serum miR-210 may be upregulated during the early stage

of clear cell renal carcinoma and can be useful for early diagnosis [20]. In addition, upregulation of certain miRNAs, including miR-21, miR-210 and miR-630, or the downregulation of certain miRNAs, including miR-126, miR-106b, miR-99a and miR-27b have been reported to be closely related with a poor prognosis of RCC [21]. Through analyzing miRNAs in tissues obtained from 203 clear cell RCC patients, Shu et al. found that decreased levels of miR-204-5p or miR-139-5p are associated with a nearly three-fold increase in the risk of recurrence ( $P<0.01$ ) [22]. In other words, these studies suggested that miRNAs play important roles in the development and progression of RCC, which allows miRNAs to function as potential biomarkers of diagnosis and prognosis.

Our research focus, miR-33b, is found in introns of the genes that encode SREBP-1 transcription factors. It performs the same function as miR-33a in cholesterol metabolism, but it exhibits a more prominent regulatory impact in mitochondrial energy homeostasis and glucose control [23]. Recently, miR-33b has been reported to participate in the disease progression of many types of neoplasms. In osteosarcoma, for instance, miR-33b suppresses glycolysis by targeting Lactate Dehydrogenase A (LDHA), which can inhibit tumor cell proliferation [24]. Additionally, low miR-33b expression has been revealed in

lung adenocarcinoma cells, while miR-33b restoration was found to suppress lung adenocarcinoma cell proliferation, invasion and migra-

**Table 5.** Target genes of miR-33b-5p matched with up-regulated DEGs of RCC

Gene Symbol	Log <sub>2</sub> (FC)	adjp
GRM8	1.054	<0.001
YWHAH	1.06	<0.001
TBX15	1.069	<0.001
SLC12A5	1.075	<0.001
PTGFRN	1.077	<0.001
SDC3	1.105	<0.001
TMEM200B	1.116	<0.001
S1PR1	1.124	<0.001
TCF4	1.199	<0.001
MAP4K4	1.228	<0.001
ANO4	1.359	<0.001
LINGO1	1.404	<0.001
ABCA1	1.436	<0.001
SH2B3	1.44	<0.001
NLGN1	1.679	<0.001
AXL	1.689	<0.001
SEL1L3	2	<0.001
LDHA	2.056	<0.001
CDH6	2.326	<0.001
VCAN	2.511	<0.001
PNMA2	2.832	<0.001

21 potential target genes are obtained. Log<sub>2</sub> (FC): Log<sub>2</sub> (Fold Change); adjp: Adjusted *p*-value.

tion. These effects may be achieved through miR-33b upregulation, which significantly reduces ZEB1 and  $\beta$ -catenin expression in lung epithelium cells [25]. Results from Lin et al. reveal lower miR-33b expression in breast tumor samples than adjacent non-tumor tissues. Non-cancerous mammary epithelial cells show an increased ability of self-renewal, migration and invasion after miR-33b knockdown. Additionally, levels of miR-33b expression were found to be inversely correlated with lymph node metastasis, which may be closely related with patient prognosis [12]. In hepatocellular carcinoma, downregulation of miR-33b has been shown in HCC tissues, while overexpression of miR-33b was found to suppress tumor cells proliferation [10]. Zhai et al. have revealed that miR-33b is downregulated in non-small cell lung cancer, while miR-33b mimic transfection suppresses its proliferation and induces apoptosis by targeting Lactate Dehydrogenase A (LDHA) [26], which is probably the same mechanism shown in osteosarcoma [24]. In brief, all these studies reveal the tumor-suppressive effects of miR-33b.

Although many studies have been conducted to explore the effects of miR-33b in several types of cancers and diseases, only few studies specifically targeted miR-33b-5p. Additionally, most of these studies are of a single original and do not provide strong evidence to illuminate the roles of miR-33b-5p. In addition, no studies have been conducted on the role of miR-33b-5p on RCC. Our research is the first study to explore the expression and functions of miR-33b-5p in RCC. The results of our study indicate that miR-33b-5p expression in RCC tissues, ACHN, 786-O and Caki-1 cells are down-regulated, compared with that of paired kidney normal tissues and HEK-293T cells, which suggests that miR-33b-5p is closely related to the development of RCC. Additionally, downregulation of miR-33b-5p has a positive effect on RCC cell proliferation, migration, invasion and inhibition of apoptosis, while upregulation of miR-33b-5p neutralizes this effect. This indicates that miR-33b-5p serves as a tumor suppressive regulator in RCC. The anti-oncogenic effects of miR-33b-5p are consistent with most previous studies. Previous studies on miR-33b have also found that it is associated with TNM stage and tumor size in colorectal cancer [11]. The survival analysis of patients with multiple myeloma show that low miR-33b expression significantly shortens progression free survival time [9].

In our study, results from TCGA and the prognostic analysis of FFPE RCC samples reveal that low miR-33b-5p expression patients have an obviously poorer survival, while patients high miR-33b-5p expression are more likely to survive. This suggests that miR-33b-5p expression level is positively correlated with the survival probability of RCC patients. Thus, miR-33b-5p may potentially function as an effective prognostic marker for RCC. Target genes prediction and TCGA database analysis suggest that TBX15 (T-Box Transcription Factor 15), SLC12A5 (Solute Carrier Family 12 Member 5), and PTGFRN (Prostaglandin F2 Receptor Inhibitor, CD9P-1) are potential targets of miR-33b-5p in RCC. TBX15 has been found to reduce cancer cell apoptosis by decreasing the proapoptotic Bax regulator and increasing the antiapoptotic Bcl2 and Bcl-XL regulators [27]. Yu. et al. revealed the potential oncogenic effect of SLC12A5 in colon cancer [28]. Furthermore, the expression level of PTGFRN positively correlates with the metastatic status of lung

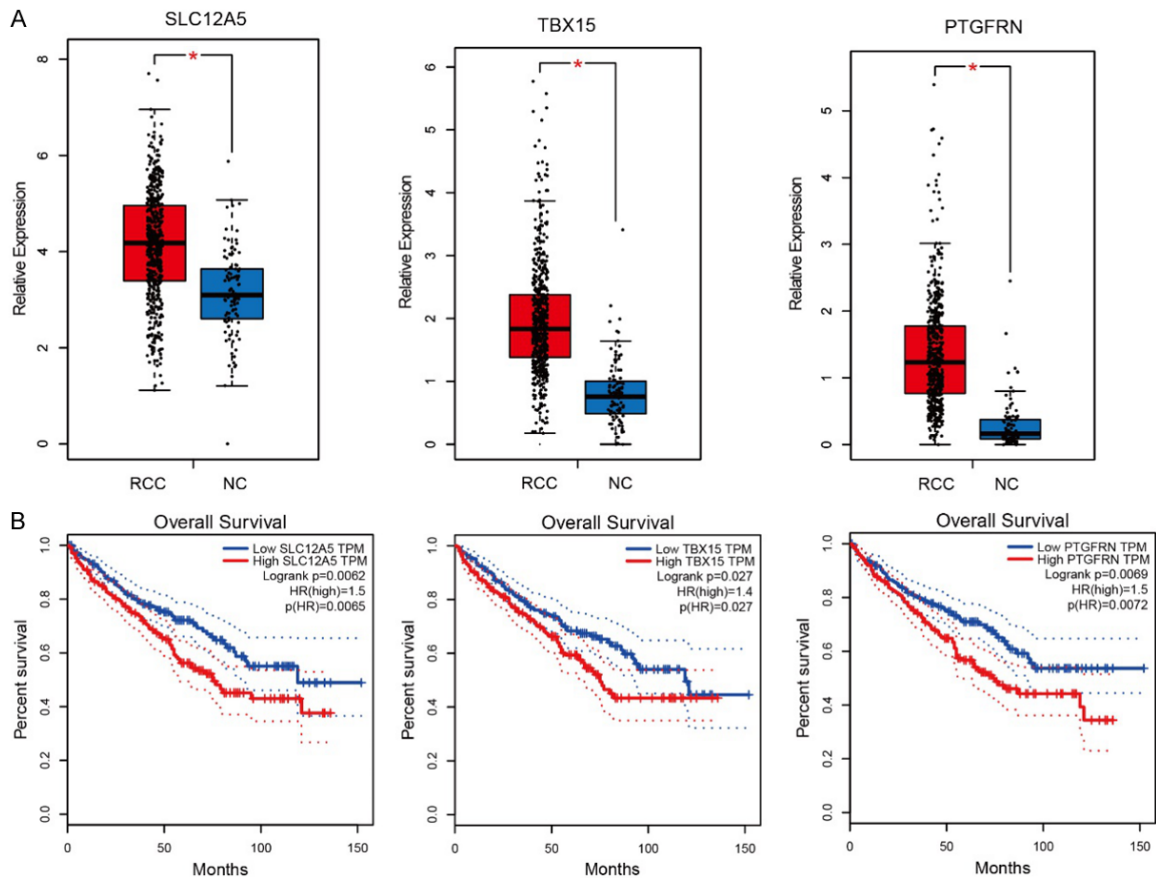


**Figure 8.** The TCGA dataset analysis of the potential target genes of miR-33b-5p. A. Relative expression levels of target genes SLC12A5, TBX15, and PTGFRN in RCC tissues. All these three genes are significantly upregulated in RCC tissues. B. Survival analysis of SLC12A5, TBX15, and PTGFRN. RCC patients with high expression levels of SLC12A5, TBX15, or PTGFRN tend to have a poor overall survival rate. \* $P < 0.05$ , \*\* $P < 0.01$ , \*\*\* $P < 0.001$ . RCC, renal cell carcinoma; NC, negative control.

cancer [29]. In this study, the expression levels of TBX15, SLC12A5, and PTGFRN are higher in RCC than NC. And up-regulation of TBX15, SLC12A5, and PTGFRN are closely related to the poor overall survival of RCC patients. Therefore, we conjecture that TBX15, SLC12A5, and PTGFRN are potential targets of miR-33b-5p to perform its tumor suppressive and prognostic effects.

The limitations of this research are that more cases should have been involved in the study and that the precise mechanism of miR-33b-5p in RCC needs to be further illuminated.

#### Acknowledgements

This study was supported by Basic Research Project of Peking University Shenzhen Hospital (JCYJ2017001, JCYJ2017004, JCYJ2017-

005, JCYJ2017006, JCYJ2017007, JCYJ2017-012), Clinical Research Project of Peking University Shenzhen Hospital (BCYJ2017001), Science and Technology Development Fund Project of Shenzhen (no. JCYJ20180507183-102747) and Clinical Research Project of Shenzhen Health Commission (no. SZLY2018-023).

#### Disclosure of conflict of interest

None.

**Address correspondence to:** Liangchao Ni and Yong-qing Lai, Guangdong and Shenzhen Key Laboratory of Male Reproductive Medicine and Genetics, Peking University Shenzhen Hospital, Shenzhen 518036, Guangdong, P. R. China. Tel: +86-0755-83923333-5862; E-mail: Incord@163.com (LCN); yqlord@163.com (YQL)

# References

- [1] Mikami S, Kuroda N and Nagashima Y. Pathology of renal cell carcinoma. In: Oya M, editor. Renal cell carcinoma: molecular features and treatment updates. Tokyo: Springer Japan; 2017. pp. 105-137.
- [2] Siegel RL, Miller KD and Jemal A. Cancer statistics, 2019. *CA Cancer J Clin* 2019; 69: 7-34.
- [3] Perazella MA, Dreicer R and Rosner MH. Renal cell carcinoma for the nephrologist. *Kidney Int* 2018; 94: 471-483.
- [4] MD BR. Renal cell carcinoma. *Ferri's Clinical Advisor* 2019. 2019. pp. 1189-1190.
- [5] Motzer RJ, Jonasch E, Agarwal N, Bhayani S, Bro WP, Chang SS, Choueiri TK, Costello BA, Derweesh IH, Fishman M, Gallagher TH, Gore JL, Hancock SL, Harrison MR, Kim W, Kyriakopoulos C, LaGrange C, Lam ET, Lau C, Michaelson MD, Olencki T, Pierorazio PM, Plimack ER, Redman BG, Shuch B, Somer B, Sonpavde G, Sosman J, Dwyer M and Kumar R. kidney cancer, version 2.2017, NCCN clinical practice guidelines in oncology. *J Natl Compr Canc Netw* 2017; 15: 804-834.
- [6] Barata PC and Rini BI. Treatment of renal cell carcinoma: current status and future directions. *CA Cancer J Clin* 2017; 67: 507-524.
- [7] Mohr AM and Mott JL. Overview of microRNA biology. *Semin Liver Dis* 2015; 35: 3-11.
- [8] Bracken CP, Scott HS and Goodall GJ. A network-biology perspective of microRNA function and dysfunction in cancer. *Nat Rev Genet* 2016; 17: 719-732.
- [9] Li F, Hao M, Feng X, Zang M, Qin Y, Yi S, Li Z, Xu Y, Zhou L, Sui W, Deng S, Zou D, Zhan F and Qiu L. Downregulated miR-33b is a novel predictor associated with disease progression and poor prognosis in multiple myeloma. *Leuk Res* 2015; 39: 793-799.
- [10] Li Y, Li R, Fu X, Zhou W, Peng S and Fu L. MicroRNA-33b inhibits cell proliferation in hepatocellular carcinoma via targeting SALL4. *Zhong Nan Da Xue Xue Bao Yi Xue Ban* 2016; 41: 905-910.
- [11] Liao W, Gu C, Huang A, Yao J and Sun R. MicroRNA-33b inhibits tumor cell growth and is associated with prognosis in colorectal cancer patients. *Clin Transl Oncol* 2016; 18: 449-456.
- [12] Lin Y, Liu AY, Fan C, Zheng H, Li Y, Zhang C, Wu S, Yu D, Huang Z, Liu F, Luo Q, Yang CJ and Ouyang G. MicroRNA-33b inhibits breast cancer metastasis by targeting HMGA2, SALL4 and Twist1. *Sci Rep* 2015; 5: 9995.
- [13] Agarwal V, Bell GW, Nam JW and Bartel DP. Predicting effective microRNA target sites in mammalian mRNAs. *Elife* 2015; 4: e05005.
- [14] Vannini I, Fanini F and Fabbri M. Emerging roles of microRNAs in cancer. *Curr Opin Genet Dev* 2018; 48: 128-133.
- [15] Hayes J, Peruzzi PP and Lawler S. MicroRNAs in cancer: biomarkers, functions and therapy. *Trends Mol Med* 2014; 20: 460-469.
- [16] Chen X, Wu L, Li D, Xu Y, Zhang L, Niu K, Kong R, Gu J, Xu Z, Chen Z and Sun J. Radiosensitizing effects of miR-18a-5p on lung cancer stem-like cells via downregulating both ATM and HIF-1alpha. *Cancer Med* 2018; 7: 3834-3847.
- [17] Fan B, Shen C, Wu M, Zhao J, Guo Q and Luo Y. miR-17-92 cluster is connected with disease progression and oxaliplatin/capecitabine chemotherapy efficacy in advanced gastric cancer patients: a preliminary study. *Medicine (Baltimore)* 2018; 97: e12007.
- [18] Hagstrom AD and Denham J. microRNAs in high and low responders to resistance training in breast cancer survivors. *Int J Sports Med* 2018; 39: 482-489.
- [19] Noorolyai S, Mokhtarzadeh A, Baghbani E, Asadi M, Baghbanzadeh Kojabad A, Mogaddam MM and Baradaran B. The role of microRNAs involved in PI3-kinase signaling pathway in colorectal cancer. *J Cell Physiol* 2019; 234: 5664-5673.
- [20] Iwamoto H, Kanda Y, Sejima T, Osaki M, Okada F and Takenaka A. Serum miR-210 as a potential biomarker of early clear cell renal cell carcinoma. *Int J Oncol* 2014; 44: 53-58.
- [21] Gu L, Li H, Chen L, Ma X, Gao Y, Li X, Zhang Y, Fan Y and Zhang X. MicroRNAs as prognostic molecular signatures in renal cell carcinoma: a systematic review and meta-analysis. *Oncotarget* 2015; 6: 32545-32560.
- [22] Shu X, Hildebrandt MA, Gu J, Tannir NM, Matin SF, Karam JA, Wood CG and Wu X. MicroRNA profiling in clear cell renal cell carcinoma tissues potentially links tumorigenesis and recurrence with obesity. *Br J Cancer* 2017; 116: 77-84.
- [23] Aryal B, Singh AK, Rotllan N, Price N and Fernandez-Hernando C. MicroRNAs and lipid metabolism. *Curr Opin Lipidol* 2017; 28: 273-280.
- [24] Zheng XM, Xu CW and Wang F. MiR-33b inhibits osteosarcoma cell proliferation through suppression of glycolysis by targeting Lactate Dehydrogenase A (LDHA). *Cell Mol Biol (Noisy-le-grand)* 2018; 64: 31-35.
- [25] Li Y, Jin L, Chen D, Liu J, Su Z, Yang S, Gui Y, Mao X, Nie G and Lai Y. Tumor suppressive miR-196a is associated with cellular migration, proliferation and apoptosis in renal cell carcinoma. *Mol Med Rep* 2016; 14: 560-566.
- [26] Zhai S, Zhao L, Lin T and Wang W. Downregulation of miR-33b promotes non-small cell lung cancer cell growth through re-

- programming glucose metabolism miR-33b regulates non-small cell lung cancer cell growth. *J Cell Biochem* 2019; 120: 6651-6660.
- [27] Arribas J, Gimenez E, Marcos R and Velazquez A. Novel antiapoptotic effect of TBX15: overexpression of TBX15 reduces apoptosis in cancer cells. *Apoptosis* 2015; 20: 1338-1346.
- [28] Yu C, Yu J, Yao X, Wu WK, Lu Y, Tang S, Li X, Bao L, Li X, Hou Y, Wu R, Jian M, Chen R, Zhang F, Xu L, Fan F, He J, Liang Q, Wang H, Hu X, He M, Zhang X, Zheng H, Li Q, Wu H, Chen Y, Yang X, Zhu S, Xu X, Yang H, Wang J, Zhang X, Sung JJ, Li Y and Wang J. Discovery of biclonal origin and a novel oncogene SLC12A5 in colon cancer by single-cell sequencing. *Cell Res* 2014; 24: 701-712.
- [29] Colin S, Guilmain W, Creoff E, Schneider C, Steverlynck C, Bongaerts M, Legrand E, Vannier JP, Muraine M, Vasse M and Al-Mahmood S. A truncated form of CD9-partner 1 (CD9P-1), GS-168AT2, potently inhibits in vivo tumour-induced angiogenesis and tumour growth. *Br J Cancer* 2011; 105: 1002-1011.